

GA-A27822

**THERMAL ION ORBIT LOSS
AND RADIAL ELECTRIC FIELD IN DIII-D**

by

J.S. deGRASSIE, J.A. BOEDO, B.A. GRIERSON, and R.J. GROEBNER

JUNE 2014



DISCLAIMER

This report was prepared as an account of work sponsored by an agency of the United States Government. Neither the United States Government nor any agency thereof, nor any of their employees, makes any warranty, express or implied, or assumes any legal liability or responsibility for the accuracy, completeness, or usefulness of any information, apparatus, product, or process disclosed, or represents that its use would not infringe privately owned rights. Reference herein to any specific commercial product, process, or service by trade name, trademark, manufacturer, or otherwise, does not necessarily constitute or imply its endorsement, recommendation, or favoring by the United States Government or any agency thereof. The views and opinions of authors expressed herein do not necessarily state or reflect those of the United States Government or any agency thereof.

GA-A27822

THERMAL ION ORBIT LOSS AND RADIAL ELECTRIC FIELD IN DIII-D

by

J.S. deGRASSIE, J.A. BOEDO,* B.A. GRIERSON,† and R.J. GROEBNER

This is a preprint of a paper to be presented at the Forty-First European Physical Society Conf. on Plasma Physics, June 23–27, 2014 in Berlin, Germany and to be published in the *Proceedings*.

*University of California San Diego, La Jolla, California 92093, USA.

†Princeton Plasma Physics Laboratory, Princeton, New Jersey 08543, USA.

Work supported in part by
the U.S. Department of Energy under
DE-FC02-04ER54698, DE-FG02-07ER54917, and DE-AC02-09CH11466

GENERAL ATOMICS PROJECT 30200
JUNE 2014



Thermal Ion Orbit Loss and Radial Electric Field in DIII-D

J.S. deGrassie¹, J.A. Boedo², B.A. Grierson³, and R.J. Groebner¹

¹General Atomics, P.O. Box 85608, San Diego, California, 92186-5608 USA

²University of California San Diego, La Jolla, California, 92093, USA

³Princeton Plasma Physics Laboratory, Princeton New Jersey 08543, USA

A simple neoclassical (NC) model for the return current balancing the thermal ion orbit loss current is consistent with measurements of the edge electric field just inside the outboard near-midplane LCFS in DIII-D. This local model has been motivated by recent Mach probe measurements of an edge co- I_p bulk ion flow layer in this region [1,2], with the velocity profile typically in agreement with a simple thermal ion orbit empty loss-cone model [2-4]. In addition, recent particle simulations have verified the existence of a steady-state ion particle distribution function (pdf) with a depleted loss cone region [5]. The probe measurements have also shown that there can be a relatively large positive radial electric field, $E_r \sim 10$ kV/m, just inside the LCFS in Ohmic conditions in DIII-D. These two emerging experimental indications, an empty loss-cone edge pdf from simulations and a significant probe-measured positive E_r in Ohmic discharges have motivated the development of this return current model. Understanding the drive for edge E_r is important as E_r shear is assumed necessary for an edge transport barrier.

The NC return current results from the E_r/B_θ precessing trapped ions undergoing friction with passing ions, where B_θ is the poloidal magnetic field strength. The empty loss cone pdf is utilized, and all the boundary regions in velocity space for trapped, passing, and lost ions are taken to depend upon the local E_r [4]. The empty loss cone pdf results in a co- I_p bulk ion velocity, U_{loss} , peaking near the outboard LCFS and decaying going inward on the scale of the poloidal ion gyroradius, $\rho_\theta = \bar{v}/\omega_\theta$, with $\bar{v} = \sqrt{T_i/M_i}$ and $\omega_\theta = Z_i e B_\theta / M_i$ [3,4]. The friction from the portion of U_{loss} carried by co-passing ions drives a return current even if $E_r = 0$. For relatively high collisionality conditions (i.e. low T_i) E_r may be positive with sufficient return current driven by $U_{\text{loss}} - E_r/B_\theta$ to balance the loss current.

For the loss current we consider only a region within roughly one ρ_θ of the LCFS, where we make the approximation that the loss cone is the relatively simple region defined by all pitch angles that allow counter- I_p starting ions to reach the X-point of a diverted discharge [3,4]. This velocity space boundary depends upon E_r , and with $E_r \neq 0$ becomes dependent on

the particle kinetic energy, $M_i v^2/2$ [4]. The velocity space sink computation is made tractable by assuming the width of the boundary layer pdf at the loss pitch angle, p_x , is given by diffusion in pitch angle taken over a parallel streaming time parameter, $\tau_{\parallel} = L_{\parallel}/|v_{\parallel}| = L_{\parallel}/|\cos(p_x)|v$, with L_{\parallel} the path length from the outboard starting point to the X-point loss. This width becomes $\sqrt{\langle \Delta \xi^2 \rangle} = \sqrt{2D_{\xi\xi}\tau_{\parallel}} = \sqrt{v_d(1-\xi^2)\tau_{\parallel}}$, with v_d the ion-ion deflection frequency and $\xi = \cos(p)$ taken at p_x . Model locality means that no gradients are included, so there are no Pfirsch-Schlüter or diamagnetic flows.

Performing the integrations over a Maxwellian pdf outside the loss cone in velocity space we obtain, for a single ion species, $j_{\text{loss}} = Z_i e n_i \rho_{\theta} v_d \tilde{\lambda} I_{\text{loss}}$ for the local loss current, with I_{loss} a dimensionless number of order unity and $\tilde{\lambda} = (\bar{v}/v_d L_{\parallel})^2 = (\text{mfp}/L_{\parallel})^{1/2}$. The return current is $J_{\text{ret}} = -Z_i e n_i \rho_{\theta} v_d f_{\text{co}} f_{\text{tr}} (\tilde{U}_{\text{loss}} + \Delta)$, with $\Delta = -E_r/B_{\theta} \bar{v} = R \partial \Phi / \partial \psi / \bar{v}$, with $\Phi = \Phi(\psi)$ the electric potential assumed constant on a poloidal-flux surface, $\tilde{U}_{\text{loss}} = U_{\text{co}}/\bar{v}$, with U_{co} the portion of U_{loss} carried by co-passing ions, and f_{co} and f_{tr} the fraction of co-passing and trapped ions; f_{co} , f_{tr} , and I_{loss} are functions of Δ . In the integrations we have approximated $v_d = v_d(\bar{v})$, while retaining the v dependence of the other integrand terms. We note that our j_{loss} agrees reasonably well with Shaing's kinetic theory calculation [6] with $\tilde{\lambda} \rightarrow 1/\sqrt{v^*}$ and Δ and ρ_{θ} used to construct an effective squeezing factor. There also can be a trapped electron contribution to j_{ret} , but for typical DIII-D edge conditions this is negligible.

Including the NC polarization current provides the equation for the temporal evolution of E_r , $\epsilon_{\text{NC}} \partial E_r / \partial t = -(j_{\text{ret}} + j_{\text{loss}})$, with $\epsilon_{\text{NC}} = n_i M_i / B_{\theta}^2$, the NC dielectric value [7]. Steady state is established on the v_d^{-1} timescale and we will apply this limit, $j_{\text{ret}}(\Delta) + j_{\text{loss}}(\Delta) = 0$. This limit neglects any time lag between j_{ret} and j_{loss} , which could lead to oscillation in E_r in the temporal equation.

In comparing with DIII-D edge data we have actually extended the above outlined derivation to include the carbon impurity because of the practical importance of $Z_{\text{eff}} > 1$ in the solutions. Despite the numerous approximations both explicit and implicit, such as using a local model for an inherently nonlocal system, we find enough agreement with the data to greatly expand these comparisons in the future. We take DIII-D EFIT equilibria, measurements of E_r , T_i , n_e , and Z_{eff} , and compute the parameters in the steady-state equation, written as $\tilde{\lambda}_1 = J_{\text{ret}}/J_{\text{loss}}$, then compare this computed value for $\tilde{\lambda}_1$ with the measurements. Here, J_{ret} and J_{loss} are scaled j_{ret} and j_{loss} with J_{ret} consisting of 4 terms for the two ion species with like and cross collisions. The scaling isolates $\tilde{\lambda}_1$ as being computed always for the main ion Z alone, for ease of comparison between different discharge conditions and

equilibria, etc. Note that $\tilde{\lambda}_1 \sim T_i$, $J_{\text{ret}} \sim \Delta \sim -E_r$, so the solutions require more negative E_r with increasing T_i [8], and this is borne out in the measured data.

A comparison of the model and data is shown in Fig. 1 for DIII-D conditions 25 ms after an H-mode transition resulting from ~ 600 kW of EC heating and ~ 500 kW of NB heating. The low power NB for CER provided the T_i , E_r , and Z_{eff} measurements. In

the region one ρ_θ inside the LCFS we find that $\tilde{\lambda}_1$ measured agrees with the model computed value. In this single null shape with the ∇B drift toward the X-point, $L_{\parallel}=20$ m. The computation is extended inside of ρ_θ to show the trend, but the assumption for the loss cone region is not valid there. The measured Δ shows a negative E_r well in this region, with $\Delta=0.4$ corresponding to $E_r \approx -13$ kV/m. The model validity is likely best for $\tilde{\lambda}_1 \sim 1$, and not for large or small values.

The sensitivity of the model to the measurements is shown in Fig. 2 where we plot contours of $\tilde{\lambda}_1$ computed versus Δ and Z_{eff} at $\tilde{\psi}=0.98$ in Fig. 1. The solid lines indicate the measured Δ and Z_{eff} from CER, the shaded region the error bars, and the contour of the measured $\tilde{\lambda}_1$ value is shown, which has $\sim \pm 10\%$ error band around it. For fixed $\tilde{\lambda}_1$, constant T_i , an increase in Z_{eff} makes E_r less negative for return current

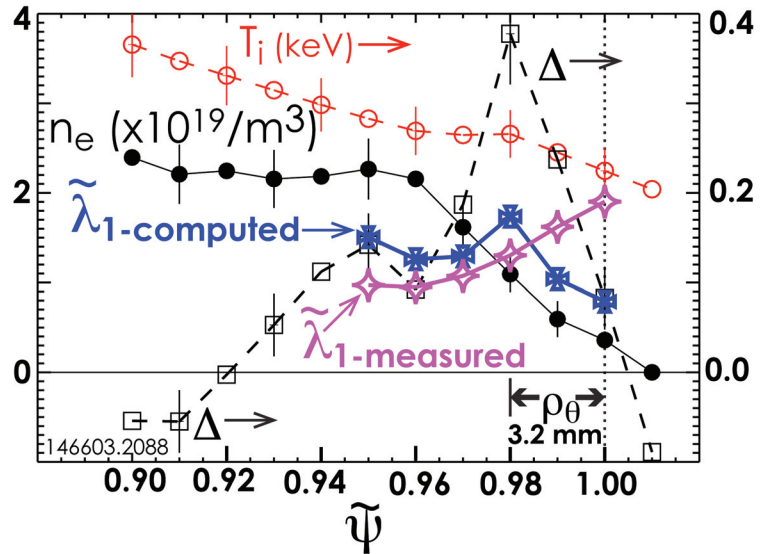


Fig. 1. Computed and measured $\tilde{\lambda}_1$, Δ , T_i , and n_e vs normalized ψ shortly after a L-H transition in DIII-D. $\tilde{\lambda}_1$ and T_i are on the right hand scale.

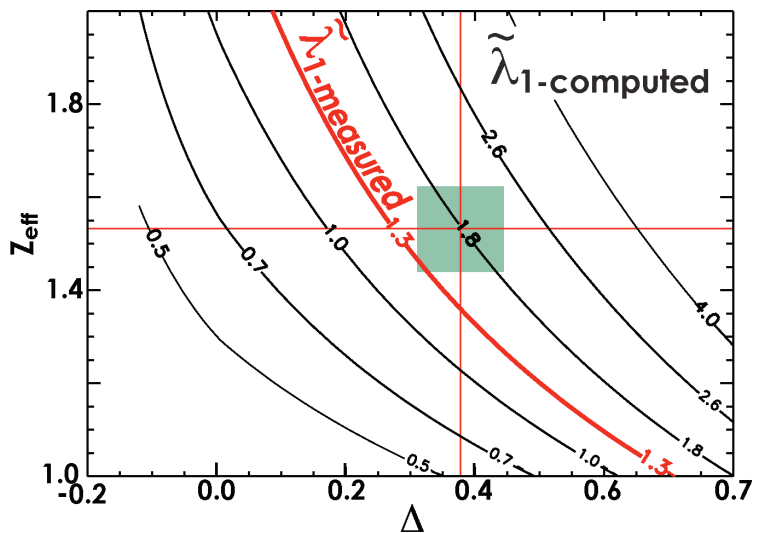


Fig. 2. Contours of $\tilde{\lambda}_1$ -computed versus Δ and Z_{eff} at $\tilde{\psi}=0.98$ with the other conditions in Fig. 1. fixed. The shaded region indicates the error bars, and the measured value contour is shown.

balance. Within the error bar limits there is a significant variation of the computed $\tilde{\lambda}_1$, nearly a factor of 2, indicating the challenge for detailed experimental verification.

A phenomenological circuit for the generation of E_r in this model is shown in Fig. 3, in the steady-state limit having $|j_{ret}| = |j_{loss}|$. For a given loss current E_r is determined by the “emf” from U_{loss} and the “orthogonal conductivity”, σ_{\perp} [9]. Other species can contribute to the two legs of the circuit, most likely perhaps fast ions in NBI or ICRF heated plasmas, through j_{loss} or the emf term.

The ion radial force balance equation must of course be satisfied on the timescale of interest. In the interior, sources of particles, energy and momentum coupled with transport determine the kinetic profiles. Then, some neoclassical or turbulence effect determines thermal ion poloidal velocity and we can use force balance to determine E_r . However, in the very edge with a dominant sink, radial current balance can determine E_r and it is probable that the least constrained quantity there is the poloidal velocity.

The evolution of the return current with heating, with increasing T_i , with the required increasingly negative E_r may be important for the L-H transition bifurcation. Measurements have shown that the shear in E_r , dE_r/dr , precedes an increase in the (negative) edge pressure gradient [10]. The natural localization of this neoclassical return current, due to the localization of the thermal loss current, provides an increasingly larger E_r shear with heating.

This work was supported by the US Department of Energy under DE-FC02-04ER54698, DE-FG02-95ER54309, DE-FG02-07AER54917, and DE-AC02-09CH11466.

- [1] J.A. Boedo et al., Phys. Plasmas **18**, 035510 (2011).
- [2] S.H. Müller et al., Phys. Rev. Lett. **106**, 115001 (2011).
- [3] J.S. deGrassie et al., Nucl. Fusion **49**, 085020 (2009).
- [4] J.S. deGrassie et al., Nucl. Fusion **52**, 013010 (2012).
- [5] D.J. Battaglia et al., Nucl. Fusion **53**, 113032 (2013).
- [6] K.C. Shaing, Phys. Fluids B **4**, 3310 (1992).
- [7] J.S. deGrassie et al., Phys. Plasmas **13**, 112507 (2006).
- [8] J.A. Heikkinen et al., Phys. Rev. Lett. **84**, 487 (2000).
- [9] Allen H. Boozer, Phys. Fluids **19**, 149 (1976).
- [10] R.A. Moyer, et al., Phys. Plasmas **2**, 2397 (1995).

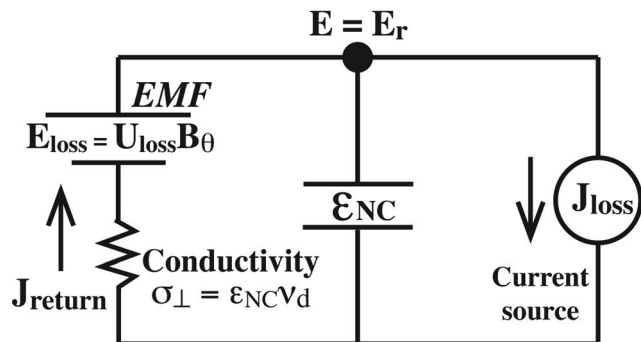


Fig. 3. Phenomenological circuit for generation of edge E_r in the “steady state” limit, $v_d t \gg 1$. U_{loss} presents an EMF, and ϵ_{NC} is the neoclassical dielectric.